ELSEVIER

Sensors and Actuators B 67 (2000) 149–160

SENSORS AND ACTUATORS B CHEMICAL

www.elsevier.nl/locate/sensorb

Microactuators toward microvalves for responsive controlled drug delivery

Lei-Mei Low, Sukeerthi Seetharaman, Ke-Qin He, Marc J. Madou*

Center for Industrial Sensors and Measurements, Department of Materials Science and Engineering, The Ohio State University, 2041 College Road, Columbus, OH 43210, USA

Received 21 June 1999; received in revised form 16 February 2000; accepted 27 February 2000

Abstract

A responsive controlled drug release system in which the delivery of drugs is achieved by actuating miniature metal or polymeric valves has been introduced. These valves might be actuated under the control of a sensor responding to a specific biological stimulus. This approach offers better reproducibility and easier control than drug release achieved by passive diffusion out of a polymer host matrix. The metal valve systems, which are irreversible, consist of thin suspended non-porous layers that can be electrochemically dissolved or disintegrated by water electrolysis. The reversible polymeric valve systems, also called 'artificial muscle', are prepared from a blend of redox polymer and hydrogel that swells and shrinks either by applying a suitable bias or through a specific chemical reaction. In one of the several possible configurations for the artificial muscle valves such as the sphincter configuration, the blend is electropolymerized within an array of holes, which open and close corresponding to the shrinking and swelling of the polymer actuator. The swelling and shrinking property of the blends is characterized by video monitoring and by in situ conductivity measurements. Significantly larger magnitude of swelling and shrinking were observed for the blend than the redox polymer itself. The blend also appeared smoother and more voluminous. The largest actuation was obtained for the blend consisting of polyaniline and poly(2-hydroxyethylmethacrylate)-poly(*N*-vinylpyrrolidinone). The results demonstrate that it is possible to apply artificial muscle for the fabrication of microactuator valves for responsive controlled drug delivery.

Keywords: Drug delivery; Valve; Redox polymer; Hydrogel; Artificial muscle; Microactuators

1. Introduction

Controlled drug release is typically achieved by encapsulating drugs in either biodegradable or nondegradable polymers, which can control the release of the drug to the body over specific duration ranging from a day to several years [1]. Although models have been developed [2,3], detailed studies on the release of drugs, including effects such as concentration-dependent diffusion and drug solubility, have been lacking due to associated complexities of the tortuous pore network in the polymer host. In order to circumvent this problem, researchers have attempted to study the release of drugs by building ordered micromachined pore networks in silicon [4].

Even though polymer drug release systems are reproducible, they are unable to respond to varying therapeutic needs of a patient because the drugs are released at a predetermined rate. Drug delivery technology could be brought to the next level by designing 'smart' polymers or devices that are 'responsive' to the patient's therapeutic requirements and deliver certain amount of a drug in response to a biological stimulus. Recent developments in biosensors and micromachining are making such controlled and responsive drug release systems possible. Controlled release systems achieved by actuating miniature valves in a drug reservoir offer the prospect of better reproducibility, ease of control, and responsive behavior. Such a micro-machined pill/Norplant drug delivery system may feature a battery, control circuitry, a biosensor, and a drug reservoir equipped with drug release actuator holes. Progress towards implementing irreversible and reversible valving schemes for the openings in the drug release systems is detailed below.

* Corresponding author. Tel.: +1-614-292-7417; fax: +1-614-688-4949.

0925-4005/00/$ - see front matter
PII: S0925-4005(00)00396-8

The study of irreversible valves has its genesis in electrorelease of drugs. Tierney and Martin [5,6] have described an electrorelease system based on microporous membranes. The molecules to be released are physically entrapped in pores of a porous membrane, which is covered in certain areas by a non-porous barrier layer material (e.g. a conductor such as Au). A second electrode is physically separated from the non-porous barrier layer that acts as a counter electrode. Release of the molecules is initiated by applying a small voltage between the barrier layer and the counter electrode and electrochemical dissolution or disruption of the barrier layer. The number of pores controls the electrorelease rate. Variation in the drug release rate may also be achieved by dividing the microporous membrane into individual electrorelease zones.

In this paper, non-porous valves in combination with Si micromachined drug release structures are described. The fabrication and application of micromachined polymer valves, or 'artificial muscle' valves, are also discussed [7]. There are several potential applications for such artificial muscle materials in micromachining such as soft microgrippers, active microfiltration, and microscopic valves and pumps for use in an 'analytical laboratory' on a chip for drug delivery or diagnostics.

The basic building materials for the artificial muscle described here are redox polymers and hydrogels. Redox polymers or conducting polymers such as polyaniline, polypyrrole, polythiophene and their derivatives have been extensively studied in the last decade. These polymers can be oxidized/reduced at moderate potentials causing changes in their physical properties such as conductivity [8], or chemical properties such as hydrophobicity [9]. The movement of counter ions and water in and out of the conducting polymer also leads to simultaneous variations in physical and electrochemical properties of the polymer such as the oxidation depth, and changes in conductivity, volume, color, etc. [10–17]. This movement is also accompanied by conformational changes along the polymeric chains, driving the opening and closing of the polymeric entanglement. Orata and Buttry [18] determined the variation in ion population and solvent content as a function of redox state and pH in polyaniline (PANI). These experiments were carried out in strong acidic solutions and revealed a change in solvent content during oxidation of the PANI. Kaneto et al. [19] described an artificial muscle based on PANI in which the proton transport in the polymer film was the driving force for the movement of the actuator. The polymer film expanded on oxidation and contracted on reduction. Similar actuator applications have also been studied for polypyrrole [20,21].

Hydrogels are considered to be the most efficient polymers in transforming molecular energy into mechanical energy. A hydrogel is a water-swollen three-dimensional network of hydrophilic homopolymers or copolymers with cross-links formed by covalent or ionic bonds [22]. Hydrogel-based actuator systems constitute an active research area in the field of robotics for building robots with noiseless and life-like movements. Various conditions such as temperature, radiation, electrical field and pH could be used to control these actuators [23]. Kurauchi [24] successfully demonstrated the electrical actuation of ionic polymer gels by creating a "gel fish" and a "gel hand". By altering the surrounding electric field, the gel fish was able to mimic swimming motion and the gel hand softly grabbed an egg.

A significant amount of work has been focused on redox polymers and hydrogels. However, the practical applications of these polymers have been limited due to some inherent difficulties. Low mechanical strength of redox polymers limits the shape and size of products that can be created. Other problems with the processibility and stability in ambient conditions have also restricted their use. In the case of gel-based actuators, the response is limited by the ability to deliver stimuli efficiently throughout the gel. Hydrogels are not electronic conductors, therefore, electro-osmotic and diffusion processes act as intermediate steps for converting electrical energy to mechanical energy in gel-based actuators. This results in low actuation rates and undesirably high working potentials [25].

This work demonstrates that combinations (blends) of hydrogels and conducting polymers can circumvent some of the problems mentioned above and create a new class of fast and efficient actuator materials. These actuators can be used in reversible polymeric valves in responsive drug delivery systems.

2. Design and fabrication

2.1. Fabrication of irreversible metal valves

A photo and a schematic of the micro fabricated Si-based drug delivery device is shown in Fig. 1. The non-porous barrier layers in the device were contacted from the back and precautions were taken to shield lead wires from exposure to fluids. A counter electrode was deposited on the front of the passivated (SiO_2) Si wafer, thereby, electrically insulating the counter electrode from the barrier layer. By applying a voltage between the barrier layer and counter electrode, the barrier layer could be electrochemically dissolved or disrupted. The Ag electrode is about 1 μm thick and Ag/AgCl is a Ag electrode with 30% converted AgCl. When a potential of +0.7 V between a Ag/AgCl counter electrode and a Ag non-porous barrier layer is applied, the barrier membrane is dissolved in a salt solution of 0.1 M NaCl or 0.1 M KCl. The rate of dissolution is proportional to the applied potential. Drug delivery chambers could also be grouped in zones. A counter electrode loop (see Fig. 1c) around a set of microchambers delineates a zone addressable by that counter electrode. Alternatively, electrodes could be addressed in-

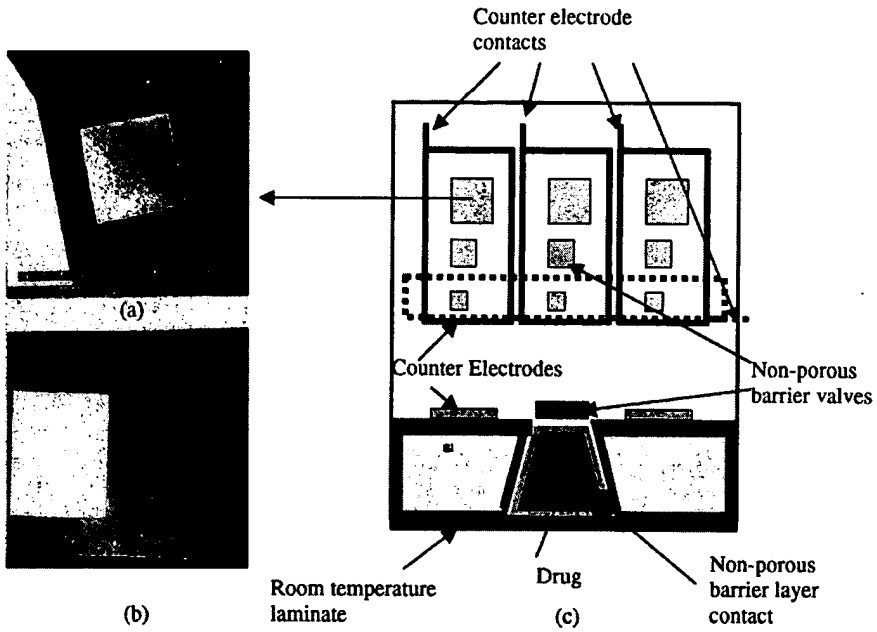

Fig. 1. (a) SEM micrograph of a 30×30 μm Pt non-porous barrier layer (anode at the bottom of a micromachined Si drug delivery cavity). (b) A Ag/AgCl and an IrO_x non-porous barrier layer in one and the same micromachined drug delivery cavity. Both electrodes are 30×30 μm. In this case, the Ag/AgCl, IrO_x electrode pair monitors the pH of the drug before release. Upon release, the Ag/AgCl is made the anode with respect to an external counter electrode. All the electrodes shown are contacted from the back of the Si wafer. (c) Non-porous barrier electrodes are blasted open electrochemically by applying a small current between the barrier material (anode) and a counter electrode (cathode) in a saline solution. Groups of micromachined cavities may contain different drugs in the same size cavities (e.g. dotted line) or the same drug in different size cavities (full line) and combinations thereof. Individual drug delivery chambers may also be addressed in an X-, Y-type fashion. The non-porous valve materials we worked with include Ag, Ag/AgCl, Pt, Au, Pd, IrO_x, etc. The liquids we experimented with (mainly hydrogels) remain enclosed in the wafer by using a room temperature laminate at the bottom of the wafer (e.g. Riston dry photoresist).

dividually in an X–Y matrix fashion. Different drugs may be stored in different zones of grouped chambers and different chamber sizes may provide different drug delivery rates. In Fig. 2, the process steps involved in fabricating a drug delivery chamber are detailed [26,27]. The fabrication of only one chamber is described here. However, since a batch process is used to fabricate the chamber, many of such identical chambers can be fabricated in parallel. In step A, a properly masked Si wafer (a ⟨100⟩ oriented wafer) was etched in a KOH solution (at 85°C) to produce the first electrochemical well. After the KOH etch, the wafer was oxidized for the first time. In step B, the properly masked wafer was etched again in KOH to create a via (cavity) from the back. The etch rate of SiO_2 in KOH is much slower than that for Si and the second KOH etch virtually stops at the moment when the etchant reaches the SiO_2 on the front side of the wafer. Thus revealing a freely suspended SiO_2 membrane. After the second KOH etching the wafer was oxidized again and the oxide layer grew thicker everywhere except on the suspended membrane, since there was no underlying Si. Metal or any desired non-porous barrier layer was then deposited from the back against the suspended oxide membrane in step C. Barrier materials such as Ag, Ag/AgCl, Au, Pt, Pd, Ti and IrO_x were investigated; however, most of the results presented here pertain to Ag, Ag/AgCl and IrO_x barrier layers. Following the deposition of the barrier layer, further timed, buffered HF etching from the front of the wafer revealed the barrier layer underneath the oxide while the rest of the wafer remained passivated with a thin oxide layer (step D).

2.2. Fabrication of reversible polymeric valves

Three different kinds of PHEMA hydrogels were prepared. The first hydrogel contained 95 wt.% 2-hydroxyethyl methacrylate (HEMA), 3 wt.% tetraethylene glycol dimethacrylate (TEGDMA) as the cross-linker, and 2 wt.% dimethoxy phenyl acetophenone (DMPA) as the photoinitiator. The second hydrogel contained 1 wt.% PVP of total weight of HEMA, in addition to all the constituents for the first hydrogel. The third hydrogel was constituted from 78.5 wt.% HEMA, 20 wt.% methyl methacrylate (MMA), 0.5 wt.% of TEGDMA per mol of MMA, and 1 wt.% DMPA.

Reagent grade aniline was vacuum distilled before application. A monomer solution of 0.1 M aniline with 0.5 M H_2SO_4 was prepared with distilled aniline and commercial reagent grade sulfuric acid. Prior to electropolymerization, the electrode was chemically cleaned in chromic acid and then electrochemically cleaned in galvanostatic mode by passing a current of ± 10 mA for 10 min.

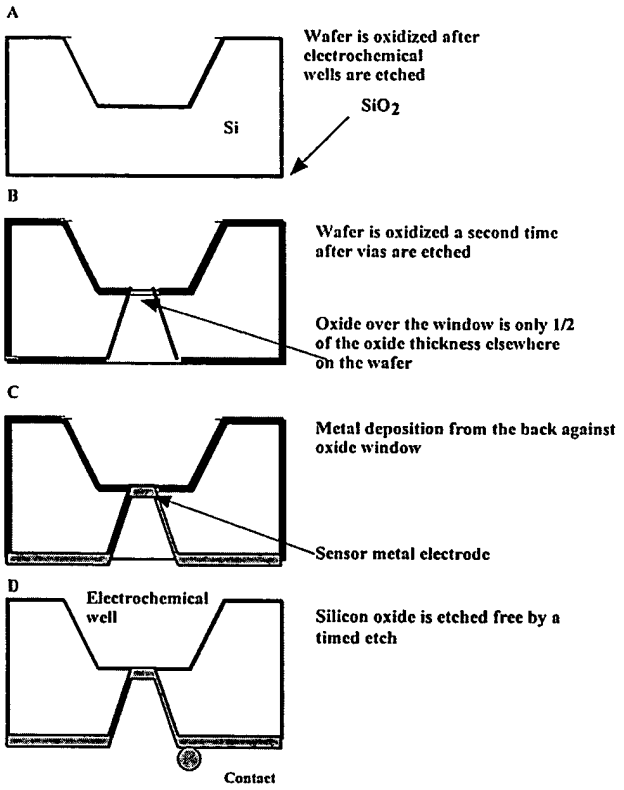

Fig. 2. Fabrication sequence for a generic drug electrorelease cell in Si. Depth of the electrochemical well, number of electrodes (barrier materials), and electrode material can all be varied.

Two different procedures were followed for electropolymerizing PANI/hydrogel on the electrode. In the first procedure, the electrode was dip coated with the hydrogel and exposed to a UV source (Blak-Ray, 270 nm) for 90 s to initiate polymerization of the hydrogel prior to initiating electropolymerization in the monomer solution (serial coating). In the second procedure, a mixture of the hydrogel and the monomer solution was simultaneously electropolymerized (parallel coating), and the PANI/hydrogel structure thus obtained was exposed to the UV source for the same duration as in the first condition. Electropolymerization was performed by cyclic voltammetry, at an electrical potential ranging from of -0.2 to $+0.8$ V (SCE) and at a scan rate of 50 mV/s, by means of a potentiostat/galvanostat (EG & G PARC model 273) controlled by CORRWARE® (Scribner Associates) electrochemistry software for a total of approximately 45 cycles, in both the procedures. The schematic of the electrochemical setup is shown in Fig. 3. The resulting structures of PANI/PHEMA artificial muscle blend were obtained following both procedures.

Three alternative designs for opening and closing holes in a drug reservoir using the artificial muscle concept are illustrated in Fig. 4. Design (a) is based on the opening and closing of an orifice by the artificial muscle in a sphincter-like mode. In design (b), the plunger configuration, the artificial muscle opens and closes a hole in a plunger-like fashion. In design (c), the tube configuration, an orifice is opened and closed laterally by the artificial muscle oozing out from a constraint tube. In all the cases, access holes enable contact between the body fluid and the muscle material. Large surface contact is required if the muscle opens and closes through a chemical stimulus from body fluids. Most of the work conducted in this research has been based on design (a).

A transmission electron microscopy (TEM) gold grid with holes of dimension 38.5×38.5 μm each (E.F. Fullam) was used as a working electrode and to simulate a substrate with an array of holes as valve seats for the artificial muscle material in a sphincter-like mode. The grid was connected to a gold lead wire of 100 μm in diameter (Alfa Aesar). To ensure good electrical and mechanical connection of the lead wire to the TEM grid, the lead wire was carefully heat bonded to the TEM gold grid. This was done by holding the grid and wire between a pair of metal tweezers and heating the tweezer over an open flame. The gold lead wire was then coated with silicone adhesive (Dow Corning) for electrical insulation.

2.3. In-situ observation and conductivity study for artificial muscle blend

Direct physical evidence regarding superior actuation properties of the blend was obtained by following the shrinking and swelling process in response to electrochemical actuation in real-time by monitoring the phenomenon with a compound microscope (NIKON ECLIPSE E-600). The microscope was connected to a video monitor, a CCD camera, a video recorder, and a color video printer (SONY). The microscope was equipped with a $20\times$ objective and $40\times$ water immersion lens. The immersion lens was chosen because of its resistance to acidic solutions and was insulated and protected from the environment by a ceramic core. The lens was immersed in 0.5 M H_2SO_4 during the monitoring process and a potential between -0.2 and $+0.8$ V (SCE) was applied to the electrode at a scan rate of 50 mV/s for a duration of 15 cycles. Real-time images of the artificial muscle were captured by the CCD camera, which was connected to the microscope. These images were viewed on the video monitor and recorded.

In order to establish a simple criteria to compare the degree of swelling and shrinking of PANI and of different artificial muscle blends prepared following the two procedures described earlier, in situ conductivity measurements were carried out for these materials. These experiments consisted of measuring the change in electrical resistance of PANI-coated and PANI/hydrogel-coated twin platinum working electrodes while switching the material from one oxidation state to the other. The twin platinum working electrodes were fabricated in the form of closely spaced wires. The distance between the two wires was approxi-

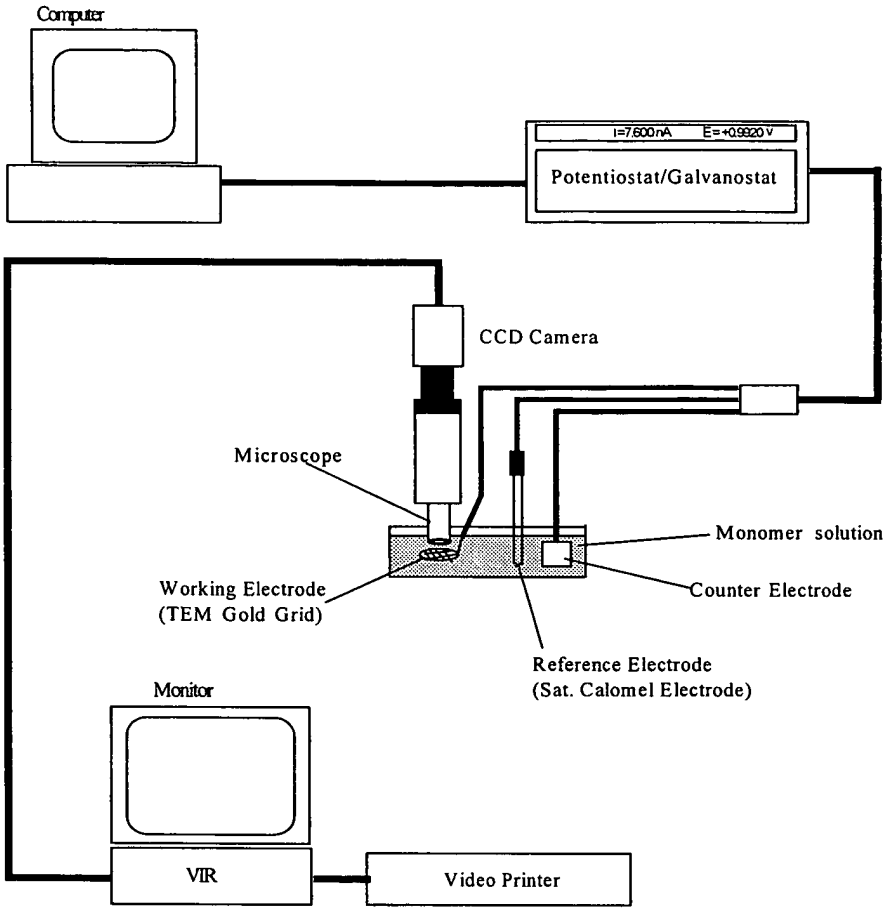

Fig. 3. Schematic of optical instrument set-up for in situ monitoring of the artificial muscle.

mately 100 μm. The PANI film and the PANI/hydrogel artificial muscle were deposited such that the gap between the wires was bridged. The schematic of the in situ conductivity measurement set-up is shown in Fig. 5. Perturbation of the channel material by applying a gate voltage causes a drain current proportional to the conductivity of the system. This assembly acts as a microelectrochemical transistor with a source and a drain connected by a channel material. In situ conductivity measurements were performed using a bi-potentiostat (PINE Instruments) by applying a potential varying between -0.2 and $+0.6$ V.

3. Results and discussion

3.1. Non-porous barrier layer valves (irreversible valves)

The initial work on micromachined non-porous barrier layers was described by Madou and Tierney [27]. In this paper, additional microfabrication details and experimental results of that work are provided. Building on the experiments conducted by Tierney and Martin [5,6], small amounts of liquids and hydrogels were enclosed into micromachined chambers in a Si substrate [26,27]. By using silicon (Si) rather than microporous membrane as a substrate, very precise and controllable integrated circuit (IC) fabrication processes can be applied to construct the Si-based drug delivery systems. The process described above is generic and is equally applicable for porous, non-porous, organic, or inorganic barrier layers. From the process illustrated in Fig. 2, it is clear that the barrier layer can be fabricated flush with the front Si surface, flush with the back surface, or be suspended anywhere in between the front and back surface. Fig. 6(a) shows a 30×30 μm Pt barrier electrode fabricated flush with the SiO_2 top surface. Fig. 6(b) shows a 30×30 μm Ag barrier electrode suspended by 200 μm below the top Si surface. The process illustrated here also allows for the fabrication of several suspended barrier layers (electrodes) in one and the same drug delivery chamber. For example in Fig. 1 (bottom left), a Ag/AgCl electrode (white electrode on the left) and an IrO_x electrode (black electrode on the right) in the same micro drug delivery chamber are shown. The IrO_x electrode is prepared by reactive sputtering from an Ir target in an oxygen/argon atmosphere. The Ag/AgCl electrode is prepared by dipping a Ag electrode (deposited by e-beam evaporation) in a ferric chloride solution. Previ-

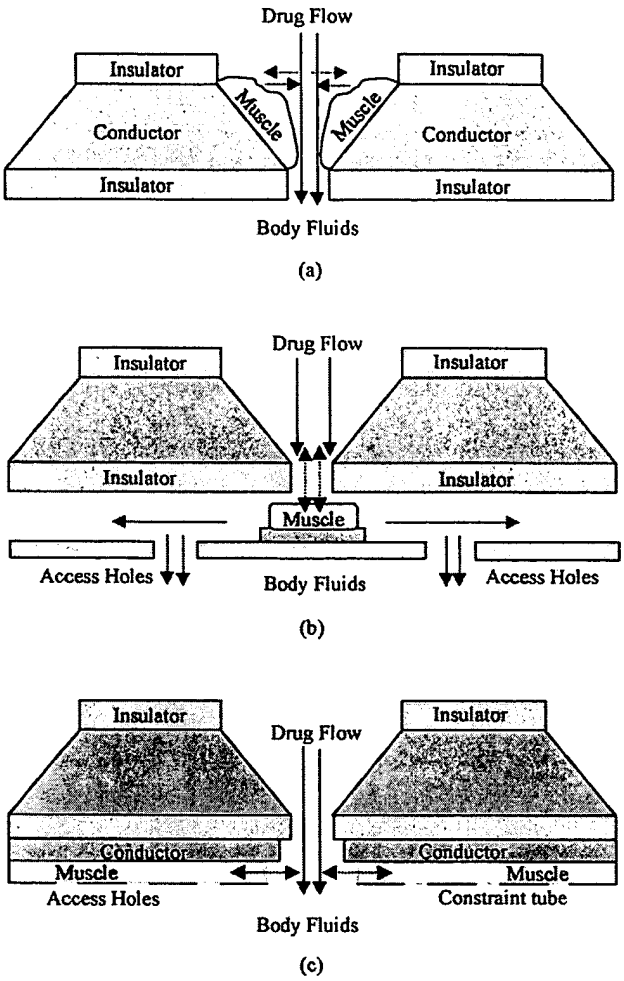

Fig. 4. Schematic of alternative designs for opening and closing holes in a drug reservoir using the artificial muscle concept. (a) Sphincter configuration (Design A); (b) Plunger configuration (design B); and (c) Tube configuration (Design C).

ously, it has been demonstrated that IrO_x is a good pH sensing metal oxide electrode [28] and by measuring the voltage between the Ag/AgCl and IrO_x electrode, the pH of the drug in the reservoir can be monitored before it is delivered into the body. Upon application of a small bias (+0.7 to +1.5 V) to the Ag/AgCl electrode (anode) vs. an external counter electrode, the Ag membrane dissolves and the drug is released. An additional chamber left unoccupied in the front of the drug release chamber that can be used for several other applications, e.g., for reacting the drug with another reagent before it is delivered into the body, for accommodating a chemical filter, for a biocompatibility layer, or for an anticoagulant, etc.

To deposit liquids (aqueous salt solutions) and hydrogels such as poly(2-hydroxyethyl methacrylate) or PHEMA and polyvinylalcohol or PVA into the micromachined cavities, experiments were conducted on drop delivery and silk-screening. Sealing the liquids and hydrogels into the wafer was achieved by applying a layer of a room temperature laminate over the back of the wafer. In this work, a dry photoresist laminate (e.g. Riston™) was used to cover the back of the Si wafer. The structure shown in Fig. 2 has also been fabricated in a variety of polymeric materials.

Our approach initiated in 1994 of using micromachining for drug delivery systems was also recently confirmed by Santini et al. [29] and Langer [30 31].

The drug release valves similar to the one shown in Fig. 1 work only once. The small current, applied between a counter electrode and the metal valve electrode, causes either dissolution of the membrane or local hydrolysis of water leading to rupturing of the thin metallic membrane.

3.2. Polymeric valves: artificial muscle (reversible valves)

In the development of a reversible polymeric valve or artificial muscle, a blend of a conducting polymer and a hydrogel was synthesized and its peculiar property of swelling and shrinking was employed to demonstrate the opening and closing of the passages in a drug reservoir. The conducting polymer in the blend forms the "electronic backbone" of the artificial muscle and is sensitive to pH, applied electrical potential, and chemical potential in its microenvironment. The hydrogel forms the "ionic body" of the muscle and exhibits dramatic effects of swelling and shrinking upon changes in pH, solvent, temperature, electric field, or ambient light conditions.

Redox polymers have been shown to attain length variations of about 30% with high reversibility. The time required to complete these variations ranges between 3 and 50 s. On the other hand, hydrogels are capable of large swelling of up to 250%; however, it takes as long as 10 to 10^4 s to complete the overall volume changes [25]. Unlike the redox polymers, the hydrogels are not redox active. Hence, a combination of the two could result in a voltage controllable material with a more impressive degree of swelling compared to a redox polymer itself. Moreover, an enhancement in the rate of swelling and shrinking in this combination could be expected because of the distribution of protons throughout the hydrogel from the redox polymer electronic backbone.

3.3. Physical chemistry

The blends investigated in this study were prepared from Polyaniline or PANI and poly(2-hydroxyethyl methacrylate) or PHEMA, the redox polymer and hydrogel, respectively. PANI was chosen because of ease in its synthesis and impressive conductivity switching properties. PHEMA is a widely studied and often used hydrogel. It is hydrostatically stable, i.e., it retains its structural integrity when subjected to swelling in water, and its permeability and hydrophilicity depend on the monomers and the type of cross-linking agents used [32]. Other copolymers that were investigated in this study include PHEMA-poly(*N*-

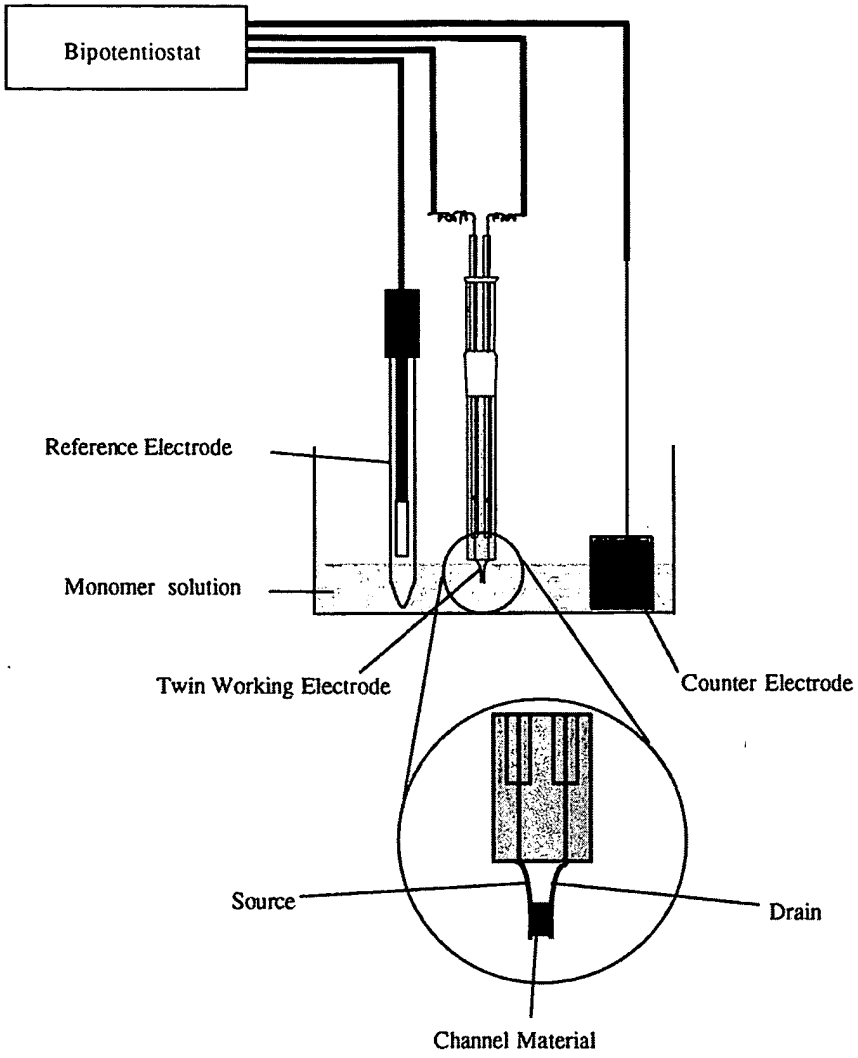

Fig. 5. Schematic of in situ conductivity measurement set-up.

vinylpyrrolidinone) or PHEMA-PVP and PHEMA-co-methyl methacrylate or PHEMA-co-MMA [33]. PVP was added to PHEMA because the addition of low-molecular weight linear polymers in the range between 1 and 5 wt.% of the organic phase has been reported to provide a more porous support that could facilitate mass transfer [34].

3.4. Artificial muscle blend morphology

It is important to characterize the artificial muscle morphology because the microfabricated valves require a smooth and uniform surface to ensure complete closure. The morphology of the conducting polymer/hydrogel artificial muscle was characterized by scanning electron microscopy (SEM). The SEM micrograph of PANI electropolymerized on a TEM gold grid is shown in Fig. 7. The PANI film was observed to be thin. The artificial muscle blend fabricated by following the serial coating procedure on a TEM gold grid is shown in Fig. 8. In contrast to PANI, the blend possessed a smooth morphology and appeared thick and voluminous. Although blends produced following serial coating procedure had smooth hydrogel structures (the open area was perfectly circular), which is important for the purpose of fabricating microactuator valves, the PANI was observed to grow only on the localized spots on the hydrogel (Fig. 9).

Synthesis of the blend following the second procedure was carried out by adding a small amount of hydrogel to the monomer solution prior to electropolymerization. Fig. 10 shows the SEM picture of PANI electropolymerized on a TEM gold grid from a mixture of monomer solution and hydrogel (parallel coating). From this figure, it can be seen that the growth of PANI on the hydrogel is more uniform.

3.5. In-situ conductivity measurements of the artificial muscle blend

Application of positive potentials to a redox polymer results in an increased influx of counterions into the polymer chains leading to enhanced swelling of the poly-

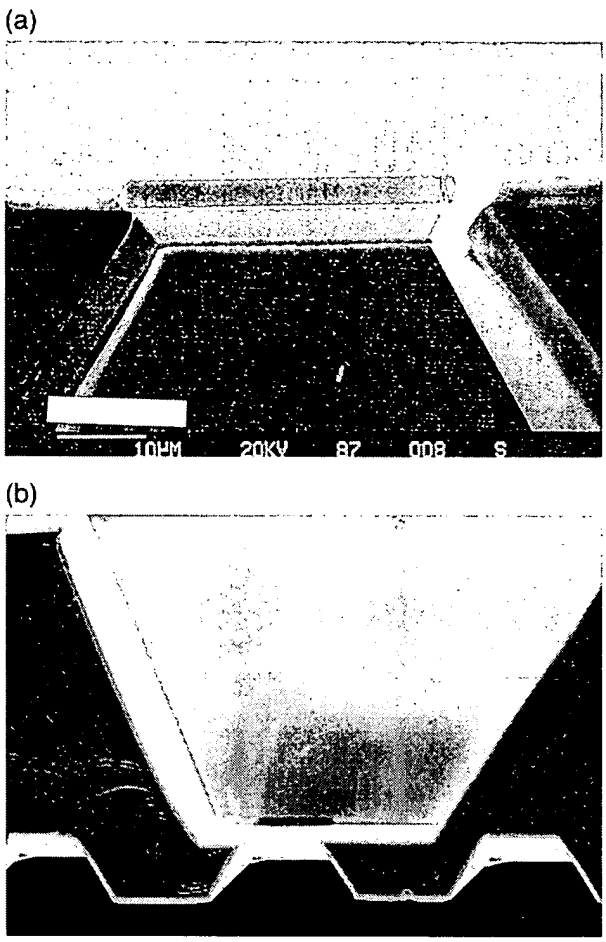

Fig. 6. SEM micrograph illustrating the result of process step D in Fig. 2. (a) A 30×30 μm Pt barrier electrode. The barrier electrode in this case is flush with the SiO_2 top surface and (b) A 30×30 μm Ag barrier electrode. The barrier electrode in this case is 200 μm deep within the wafer leaving reservoirs on both sides of the barrier material. The thinned wafer is 250 μm in total thickness.

Fig. 7. SEM micrograph of polyaniline coated TEM gold grid.

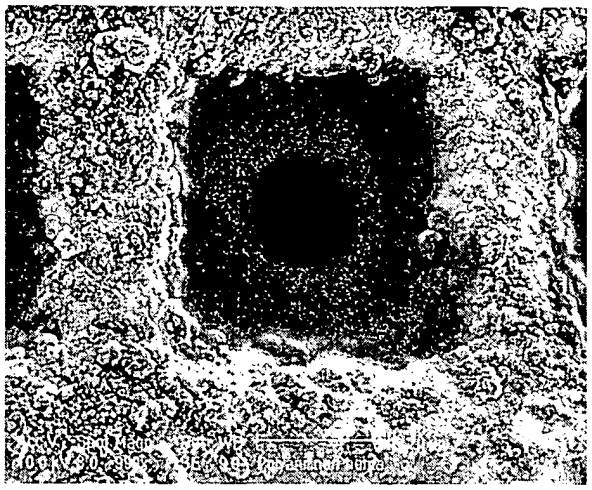

Fig. 8. SEM micrograph of polyaniline grown on TEM gold grid coated with Poly-HEMA.

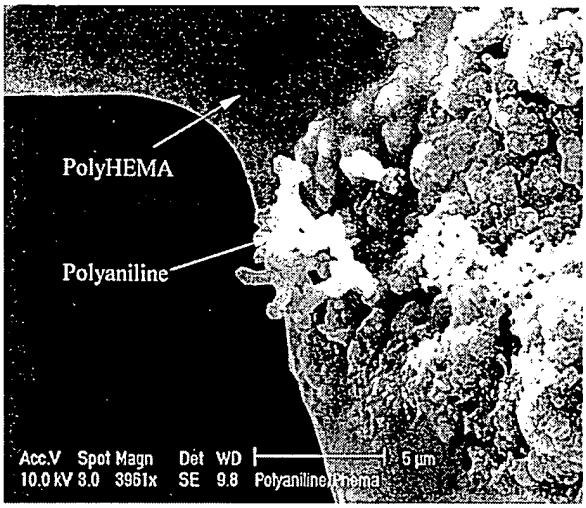

Fig. 9. SEM micrograph showing non-uniform growth of polyaniline on poly-HEMA.

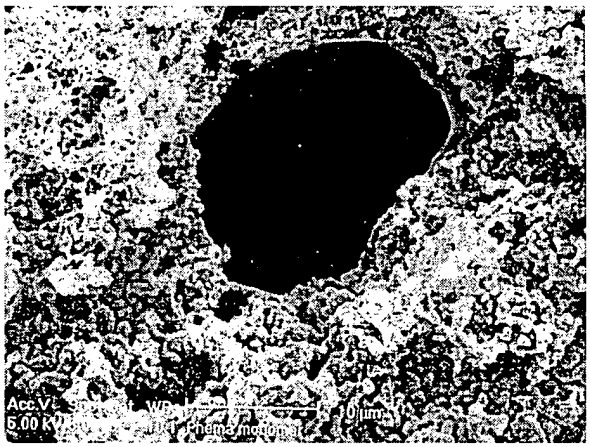

Fig. 10. SEM micrograph showing uniform growth of polyaniline on TEM gold grid from a mixture of monomer solution and hydrogel.

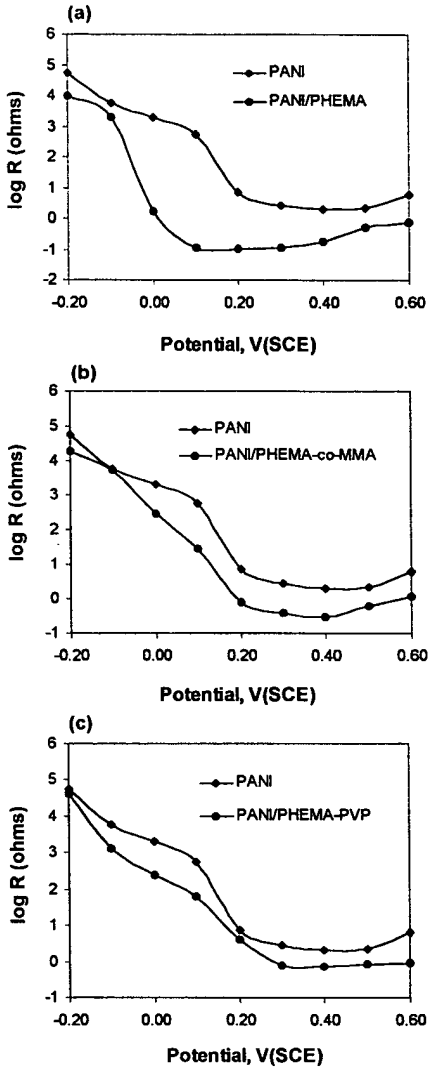

Fig. 11. Plots of log R as a function of potential, V (SCE) for (a) PANI and PANI/PHEMA blend, (b) PANI and PANI/PHEMA-co-MMA blend and (c) PANI and PANI/PHEMA-PVP blend electropolymerized following the first procedure (serial coating).

mer matrix and an increase in its conductivity or a decrease in its resistance. Hydrogels exhibit a similar behavior. Ionization of hydrogels lead to changes in their hydration as a result of electrostatic and osmotic forces that draw counterions and water into the hydrogel structure. An increase in the swelling of the hydrogel also leads to an increase in its electrical conductivity [35]. Vacik and Kopecek [36] measured the specific resistance of anionic, cationic, and ampholytic copolymer hydrogels based on 2-hydroxyethyl methacrylate as a function of pH and copolymer compositions. Their studies demonstrated that the swelling of the hydrogels results in a decrease in the specific resistance of the material. Thus, measurements of electrical conductivity could represent the extent of swelling of these materials.

The degree of swelling/shrinking of the material is related to the ratio of the resistance of the material in the conducting state and in the insulating state according to the relationship given below:

$$\text{Swelling/Shrinking} \propto \frac{\text{Lowest Resistance of the material}}{\text{Highest Resistance of the material}} \quad (1)$$

where the highest resistance corresponds to the resistance of the material at a potential of -0.2 V (SCE) or when the material is most insulating and the lowest resistance corresponds to the resistance of the material at a potential of approximately $+0.3$ V (SCE) or when the material is most conducting. This ratio is also known as the switching factor of the material. A higher value of the switching factor corresponds to a higher extent of swelling exhibited by the material.

The conductivity measurement results are plotted in Figs. 11 and 12 for the artificial muscle blends synthesized

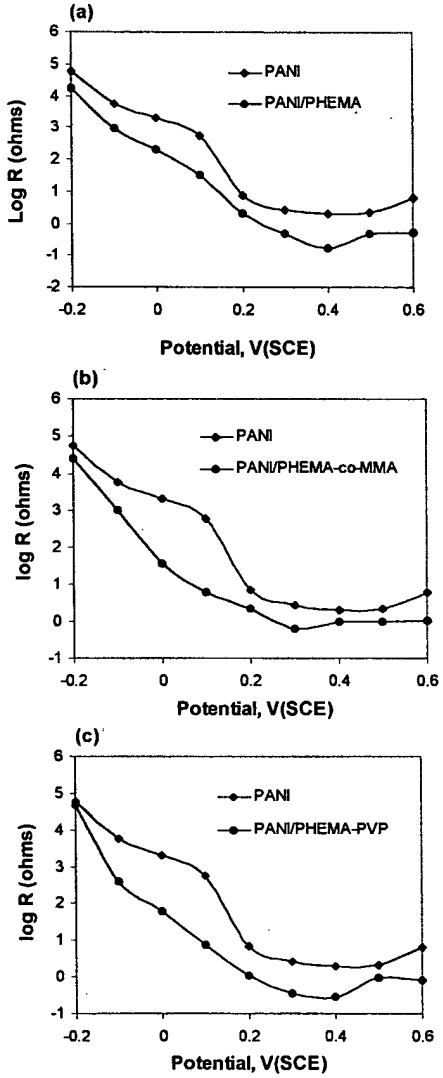

Fig. 12. Plots of log R as a function of potential, V (SCE) for (a) PANI and PANI/PHEMA blend, (b) PANI and PANI/PHEMA-co-MMA blend and (c) PANI and PANI/PHEMA-PVP blend electropolymerized following the second procedure (parallel coating).

Table 1
Switching ability of polyaniline/hydrogel blend

	$R_{-0.2\,V}/R_{+0.3\,V}$
PANI only	28840.3
Electrode coated with hydrogel prior to polymerization (serial coating)	
PANI/PHEMA	95499.3
PANI/PHEMA-co-MMA	58884.4
PANI/PHEMA-PVP	57544.0
Hydrogel dispersed in monomer solution (parallel coating)	
PANI/PHEMA	102329.3
PANI/PHEMA-co-MMA	40738.0
PANI/PHEMA-PVP	162181.0

following serial coating and parallel coating procedures, respectively. For comparison, the resistance–potential curve for PANI alone is also included in the plots.

By assuming that the proportionality constants are the same for all the polymers, the switching factors were calculated for various blends and PANI using the relationship given in Eq. 1. The calculated switching factors for PANI and various blends are tabulated in Table 1. From these values, it can be concluded that the degree of shrinking and swelling of the blend is enhanced by a factor of 5.6, from 2.9×10^4 for PANI alone to 1.6×10^5 for the blend consisting of PANI and PHEMA-PVP. Furthermore, the blend obtained by parallel coating yielded a higher switching factor, i.e., a higher degree of swelling and shrinking, than the blend prepared by serial coating. This implies that a uniform growth of PANI obtained during parallel coating is critical for achieving a higher degree of swelling and shrinking.

3.6. *In-situ monitoring of swelling and shrinking of the artificial muscle blend*

The in-situ monitoring of the artificial muscle blend of PANI and PHEMA-PVP synthesized by parallel coating showed a significant change in the size of the opening when the blend was subjected to a cyclic potential scan, as shown in Fig. 13(a) and (b). The change in the maximum cord length between the largest opening (shrunken state)

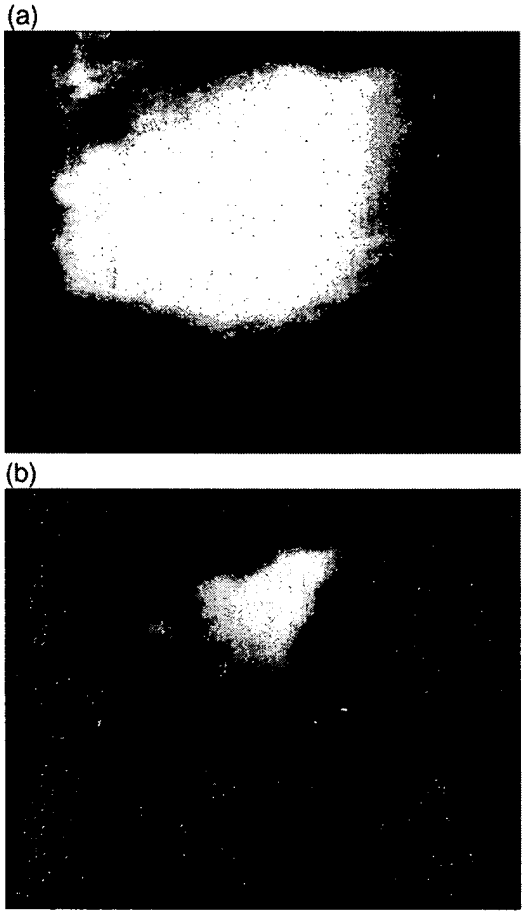

Fig. 13. Artificial muscle blend at (a) shrunken (open) state at −0.2 V (SCE) and (b) swollen (closed) state at +0.3 V (SCE). Dramatic change in the size of the hole is observed.

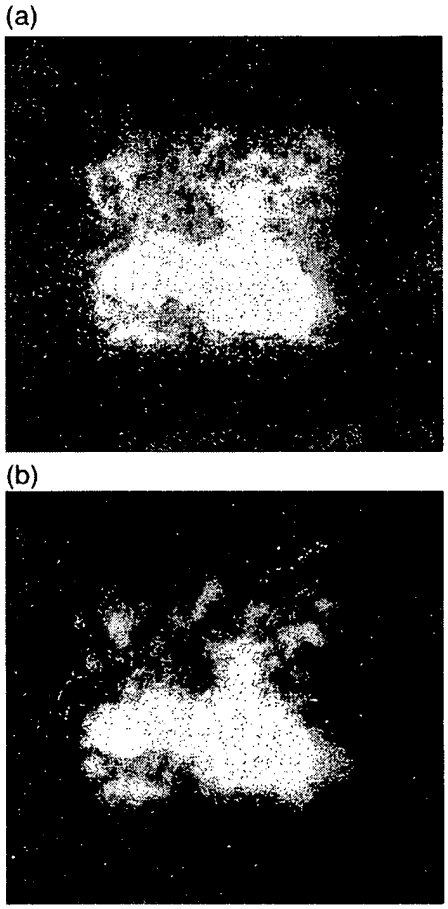

Fig. 14. Polyaniline at (a) −0.2 V (SCE) and at (b) +0.3 V (SCE). No significant change in the size of the hole is observed.

and the smallest opening (swollen state) was observed to be approximately 150%.

For comparison, real-time swelling and shrinking behavior of PANI was also examined. As can be seen from Fig. 14(a) and (b), under identical experimental conditions, no significant change in the size of the opening was observed for PANI.

4. Conclusion

In this study, non-porous barrier layer and polymeric valves for applications in a novel responsive drug delivery system were microfabricated. The non-porous barrier layer valves were irreversible and application of a small current between a counter electrode and the metal valve electrode led to rupture of the thin metallic barrier layer. The reversible polymeric valves consisting of a blend of redox polymer (PANI) and hydrogel (PHEMA-based) were also prepared to demonstrate and characterize their actuator-like properties.

The redox polymer/hydrogel blends are voluminous and have smoother morphology compared to redox polymer itself. The blends produced by following the parallel coating procedure show uniform redox polymer growth. The direct physical evidence regarding the superior actuation properties of the redox polymer/hydrogel blend is obtained by video monitoring (real-time imagery) the shrinking and swelling of the blend. In situ conductivity measurements also confirm an enhancement in the degree of shrinking and swelling of the artificial muscle blend as compared to redox polymer itself.

The novel material obtained from blending a redox polymer and a hydrogel possess qualities of a high swelling hydrogel and a voltage controllable redox polymer. Due to these qualities, this material demonstrates larger magnitude of swelling and shrinking compared to the redox polymer and a faster response time than the hydrogel. This novel material could be effectively used to fabricate microactuators or microvalves for various applications including responsive drug delivery.

We are envisioning the use of these polymer actuators in a micromachined drug delivery system. Such a micromachined pill/Norplant drug delivery system may feature a battery, control circuitry, a biosensor, and a drug reservoir equipped with drug release actuator holes.

Acknowledgements

The authors would like to acknowledge Dr. Yao Sheng and Dr. Yun-Shu Zhang for their valuable suggestions and insights. The authors would also like to acknowledge Mr. Cameron Begg and Mr. Steve Bright for their valuable assistance in conducting optical analyses.

References

[1] J. Kost, R. Langer, Responsive polymer systems for controlled delivery of therapeutics, Trends Biotechnol. 10 (1992) 127–131.
[2] A.C. Balasz, D.F. Calef, J.M. Deutch, R.A. Siegel, R.S. Langer, Biophys. J. 47 (1985) 97–104.
[3] R.A. Siegel, R. Langer, J. Coll. Int. Sci. 109 (1986) 426–440.
[4] N.F. Sheppard, D.J. Mears, S.W. Straka, Micromachined silicon structures for modeling polymer matrix controlled release systems, J. Controlled Release 42 (1996) 15–24.
[5] M.J. Tierney, C.R. Martin, Electroreleasing composite membranes for delivery of insulin and other biomacromolecules, J. Electrochem. Soc. 137 (6) (1990) 2005–2006.
[6] M.J. Tierney, C.R. Martin, New electrorelease systems based on microporous membranes, J. Electrochem. Soc. 137 (12) (1990) 3789–3793.
[7] T.W. Lewis, S.E. Moulton, G.M. Spinks, G.G. Wallace, Development of an all polymer electromechanical actuator, Synth. Met. 85 (1997) 1419–1420.
[8] A. Talaie, G.G. Wallace, The effect of the counterions on the electrochemical properties of conducting polymers — A study using resistometry, Synth. Met. 63 (2) (1994) 83–88.
[9] H. Ge, G.G. Wallace, Ion-exchange properties of polypyrrole, React. Polym. 18 (2) (1992) 133–140.
[10] K. Naoi, M.M. Lien, W.H. Smyrl, Quartz crystal microbalance study — ionic motion across conducting polymers, J. Electrochem. Soc. 138 (2) (1991) 440–445.
[11] Y.J. Qiu, J.R. Reynolds, Dopant anion controlled ion-exchange behavior of polypyrrole, Polym. Eng. Sci. 31 (6) (1991) 417–421.
[12] J.R. Reynolds, M. Pyo, Y.J. Qiu, Cation and anion dominated ion-transport during electrochemical switching of polypyrrole controlled by polymer–ion interactions, Synth. Met. 55 (2–3) (1993) 1388–1395.
[13] A.R. Hillman, M.J. Swann, S. Bruckenstein, Ion and solvent transfer accompanying polybithiophene doping and undoping, J. Electroanal. Chem. 291 (1-2) (1990) 147–162.
[14] P. Marque, J. Roncali, Structural effect on the redox thermodynamics of poly(thiophenes), J. Phys. Chem. 94 (23) (1990) 8614–8617.
[15] L.W. Shacklette, R.H. Baughman, Defect generation and charge transport in polyaniline, Mol. Cryst. Liq. Cryst. 189 (1990) 193–212.
[16] A.F. Diaz, J.I. Castillo, J.A. Logan, W.-Y. Lee, Electrochemistry of conducting polypyrrole films, J. Electroanal. Chem. 129 (1981) 115.
[17] F. Garnier, G. Tourillon, Organic conducting polymers derived from substituted thiophenes as electrochromic material, J. Electroanal. Chem. 148 (1983) 299.
[18] D. Orata, D.A. Buttry, Determination of ion populations and solvent content as functions of redox state and pH in polyaniline, J. Am. Chem. Soc. 109 (1987) 3574.
[19] K. Kaneto, M. Kaneko, Y. Min, A.G. MacDiarmid, Artificial muscle-electromechanical actuators using polyaniline films, Synth. Met. 71 (1-3) (1995) 2211–2212.
[20] T.F. Otero, J.M. Sansinena, Artificial muscle based on conducting polymers, Bioelectrochem. Bioenerg. 38 (1995) 411–414.
[21] T.F. Otero, J.M. Sansinena, Bilayer dimensions and movement in artificial muscles, Bioelectrochem. Bioenerg. 42 (1997) 117–122.
[22] N.A. Peppas, A.G. Mikos, in: Hydrogels in Medicine and Pharmacy vol. 1 CRC Press, Boca Raton, FL, 1986, p. 1.
[23] Y.M. Lee, S.H. Kim, C.S. Cho, Synthesis and swelling characteristics of pH and thermoresponsive interpenetrating polymer network hydrogel composed of poly-(vinyl alcohol) and poly(acrylic acid), J. App. Polym. Sci. 62 (2) (1996) 301–311.
[24] N. Kurauchi, Kagaku to Kyoiku 39 (1991) 618.
[25] T.A. Skotheim, R.L. Elsenbaumer, J.R. Reynolds (Eds.), Handbook of Conducting Polymers, Marcel Dekker, 1998, pp. 1015–1017.
[26] M.J. Madou, Fundamentals of Microfabrication, CRC Press, Boca Raton, FL, 1997.

[27] M.J. Madou, M.J. Tierney, Micro-Electrochemical Valves and Methods, US Patent, 5,304,293 (1994).
[28] M.J. Madou, S.R. Morrison, Chemical Sensing with Solid State Devices, Academic Press, 1989.
[29] J.T. Santini Jr., M.J. Cima, R. Langer, A controlled-release microchip, Nature (1999) 335.
[30] R. Langer, Microchips could simplify drug therapy, USA Today (1999) January 28.
[31] R. Langer, Time Mag. (1999) 52, February 8.
[32] N.A. Peppas, A.G. Mikos, in: Hydrogels in Medicine and Pharmacy vol. III CRC Press, Boca Raton, FL, 1986, p. 98.
[33] C.S. Brazel, N.A. Peppas, On the mechanisms of water transport and drug release from swellable hydrogels, Polym. Mater. Sci. Eng. Proc. 74 (1996) 370–371.
[34] G.F. Bickerstaff (Ed.), Methods in Biotechnology vol. 1 Humana Press, Clifton, NJ, 1997, p. 67.
[35] M.J. Lesho, N.F. Sheppard Jr., A method for studying swelling kinetics based on measurement of electrical conductivity, Polym. Gels Networks 5 (1997) 503–523.
[36] J. Vacik, J. Kopecek, Specific resistances of hydrophillic membranes containing ionogenic groups, J. Appl. Polym. Sci. 19 (1975) 3029–3044.